

# Boundary layer ozone and cloud coverage at Paramaribo Station (5.8N 55.2W)

*Stijn Maas*

Koninklijk Nederlands Meteorologisch Instituut

**Technical report = technisch rapport; TR-264**

De Bilt, 2004

PO Box 201  
3730 AE De Bilt  
Wilhelminalaan 10  
De Bilt  
The Netherlands  
<http://www.knmi.nl>  
Telephone +31(0)30-220 69 11  
Telefax +31(0)30-221 04 07

Author: Maas, S.  
Stageverslag [student TU/e]

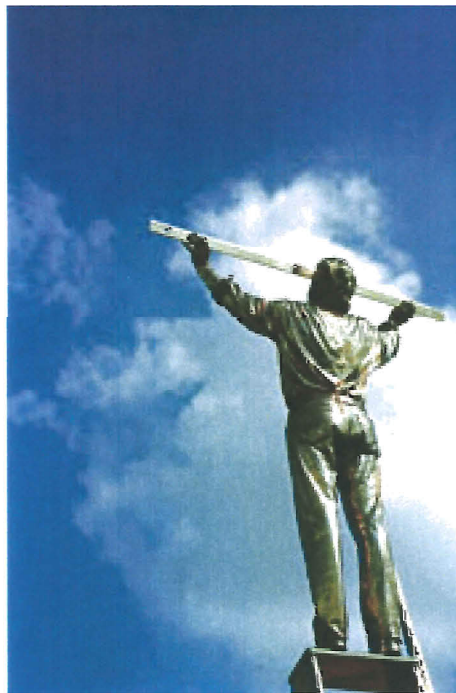
UDC: 551.510.42  
551.510.522  
551.576.2  
(883)

ISSN: 0169-1708

ISBN: 90-369-2252-6



Boundary Layer Ozone & Cloud  
Coverage at Paramaribo station  
5.8N 55.2W



Stijn Maas

Cover

The man who measures the clouds, statue by J. Fabre ©

## Abstract

This report covers the first results of two new parameters measured at the paramaribo station after the latest extension of the site.

The first parameter is the surface ozone. The results show different patterns according to the seasonal, daily and diurnal variations of the ozone mixing ratio at the surface. The surface ozone mixing ratio strongly depends on a diurnal cycle. This cycle is a result of photochemical reactions and the formation and collapse of the daytime convective boundary layer.

The monthly averaged ozone mixing ratio varies with the seasons. During the wet season a decrease of surface ozone is observed, while during the dry seasons an increase of surface ozone is observed. This could be a result of the more frequently wash-out of ozone and precursors of ozone, a better vertical mixing and less effective photochemical reactions during the wet season.

The second parameter measured is the cloud coverage. Two objective measurement methods i.e. the Total Sky Imager and the Radiation Station, are compared. The cloud coverage measurements made with TSI and the derived cloud coverage of the RS are in good accordance. The diurnal dynamics of the cloud coverage are also typical for tropical areas.

The two new measuring instruments give good results. They give reliable data output and form a great asset to the Paramaribo station. More extensive research using these new measurements and the ones already performed at the station will improve the understanding of the tropical atmosphere.



# Contents

<b>Preface</b>	<b>1</b>
<b>1 Introduction</b>	<b>3</b>
1.1 Location . . . . .	3
1.2 Climatology of Paramaribo . . . . .	4
<b>2 Boundary layer ozone</b>	<b>7</b>
2.1 introduction . . . . .	7
2.2 Main chemical ozone reaction mechanism . . . . .	8
2.2.1 Tropospheric ozone production . . . . .	8
2.2.2 Tropospheric ozone destruction . . . . .	9
2.3 Measurement technique . . . . .	9
2.4 Results . . . . .	11
2.4.1 Diurnal variations . . . . .	11
2.4.2 Day-to-day variations . . . . .	13
2.4.3 Seasonal variations . . . . .	13
2.5 Discussion and Conclusion . . . . .	15
<b>3 Cloud Coverage</b>	<b>17</b>
3.1 Introduction . . . . .	17
3.2 Measurement techniques . . . . .	18
3.2.1 traditional method . . . . .	18
3.2.2 Total Sky Imager . . . . .	18
3.2.3 Solar Radiation Station . . . . .	19
3.3 Results . . . . .	19
3.3.1 Comparison TSI-RS . . . . .	19
3.3.2 Diurnal variation . . . . .	20
3.4 Discussion and Conclusion . . . . .	21
<b>Bibliography</b>	<b>23</b>
<b>Appendix</b>	<b>25</b>





# Preface

Exploring the world of science outside the university is a significant part of the master's course applied physics at the Eindhoven University of Technology. This is the aim of the external internship. The research done during this internship described in this paper took partly place at the Royal Netherlands Meteorological Institute (KNMI) and the Meteorological Service Surinam (MDS).

The subject of this research is the boundary layer ozone and the cloud coverage at Paramaribo station.

This paper is written in  $\text{\LaTeX}$  using the native editor WinEdt 5.3. The data analysis were done in Microcal Origin 6.0.

This traineeship would have been much less instructive without the pleasant coaching of dr Gé Verver and the supervising of Prof. dr. H. Kelder from the KNMI. Other people of the KS/AS group of KNMI I like to thank are R. Scheele for modelling the trajectories and P. Fortuin for initiating this traineeship. I also would like to thank the people at MDS for their friendly cooperation during my stay in Surinam especially Mr C. Becker for his helpful and interesting discussions. This internship has been made possible with the financial support of the "J. Tindenberg" scholarship of the Nuffic institute, the Hague.

And last but certainly not least thanks to David ("Laterrr") and Katrien for their hospitality and pleasant trips and pastimes in Surinam. And Geert thanks for the moral support.



# Chapter 1

## Introduction

The tropics play an important role in the climate of the Earth, affecting the climate on a global scale. Unfortunately there are not sufficient observation stations for atmospheric parameters in the tropical regions. One of the rare stations that measures atmospheric composition, clouds and radiation is the Paramaribo station located at 5.8 N and 55.2W. In 1999 KNMI and MDS started an atmospheric observation program at this location.

The objective of this program is to provide high quality observational data on atmospheric composition and dynamics. This research is embedded in the program and is a result of the latest extensions at the site. The station's instrumentation now consists of a Brewer MKIII double spectrophotometer, a multi-axis DOAS instrument, a sunphotometer, a short-wave solar radiation station, an in-situ ozone monitor and a total sky imager. The station also runs a program of weekly ozone- and radio-soundings.

### 1.1 Location

Paramaribo, the capital of Suriname, one of the Guyana-countries is located at the northern coast of South America. It is the biggest city of Surinam, with a population of 300.000 compared to the total 400.000 inhabitants of Surinam. The city is situated at the banks of the Surinam river and is stretched out over an area of 100 square km. There is little industrial activity in and near the city. The only real source of air pollution in this area is the outdated car park.

The station is situated at the edge of the city. The direct environment consist of mangrove bushes. No sources of air pollution are located in the direct environment of the station (figure 1.1).



Figure 1.1: Paramaribo station and direct environment

## 1.2 Climatology of Paramaribo

Surinam has a typical rain forest climate . Locally the precipitation can be just below the minimum value as defined for a tropical climate (60 mm in the driest month). The average year temperature in Paramaribo is  $27,3^{\circ}$  C. The daily average maximum temperature is the highest in October ( $33,0^{\circ}$  C) and the lowest in January ( $29,8^{\circ}$  C). During the whole year, the average minimum temperature measures ca.  $23^{\circ}$  C. The relative humidity on an annual base is 80% and on average 60% of the sky is covered with clouds.

The seasons in Surinam are determined by the annual migration of the Inter Tropical Convergence Zone (ITCZ) [8]. The distinction between the wet and dry seasons is related to the position of the ITCZ. The wet seasons (December-January and April-July) correspond with the period when the ITCZ is mainly located above Surinam.

During the dry seasons (February-March and August-November) the ITCZ is located south (Feb-Mar) or north (Aug-Nov) of Surinam. During the second dry season the air transported to Surinam comes from the Southern Hemisphere. From a meteorological point of view, Surinam is located in the Southern Hemisphere during this long dry season. The migration of the ITCZ over Surinam (red spot) is shown in figure 1.2.

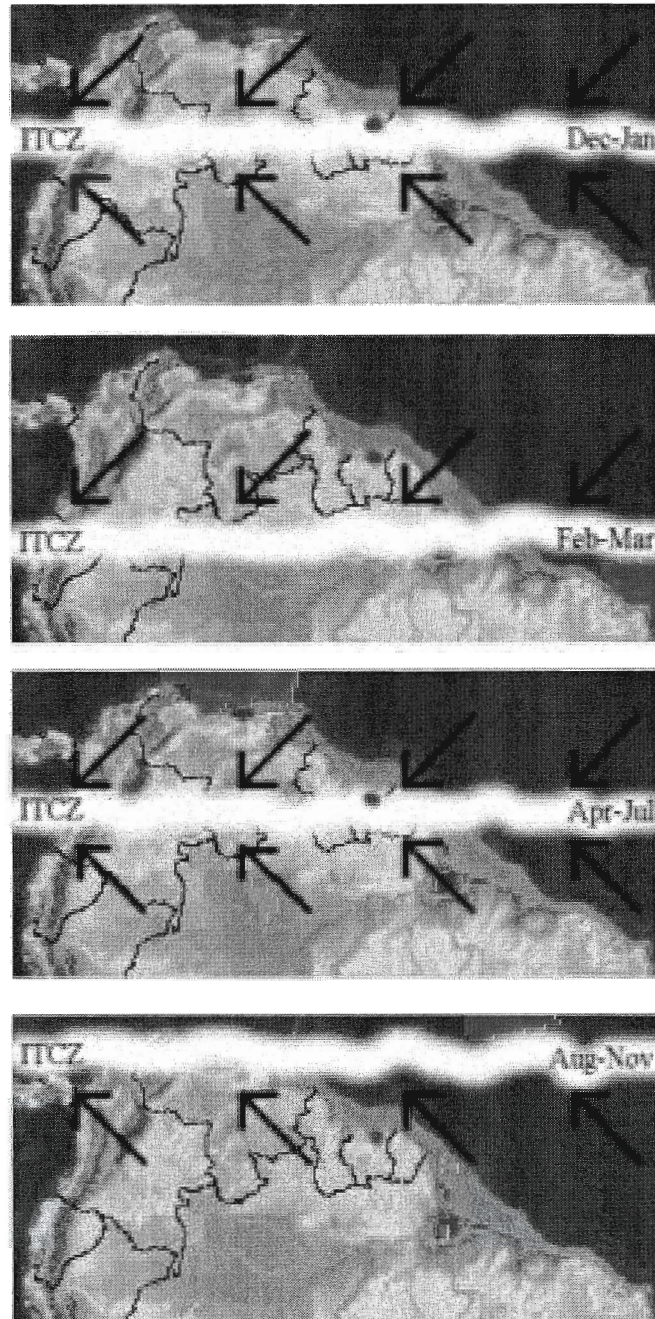


Figure 1.2: migration of ITCZ over Paramaribo



## Chapter 2

# Boundary layer ozone

### 2.1 introduction

Ozone is very rare in our atmosphere, averaging about three molecules of ozone for every 10 million air molecules. In spite of this small amount, ozone plays a vital role in the atmosphere. Ozone is mainly found in two regions of the earth's atmosphere. Most ozone (about 90%) resides in the stratosphere (between 10 and 50 km above the Earth's surface). This is called the ozone layer. The remaining ozone is found in the troposphere.

The ozone in these two regions has different effects on life forms [6]. The ozone in the ozone layer plays a beneficial role by absorbing most of the biological damaging ultraviolet sunlight (UV-B), allowing only a small amount to reach the Earth's surface. Without the filtering action of the ozone layer, more of the sun's UV-B radiation would penetrate the atmosphere and would reach the surface. Many experimental studies of plants and animals and clinical studies of humans have shown the harmful effects of excessive exposure to UV-B radiation.

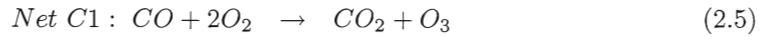
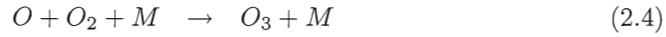
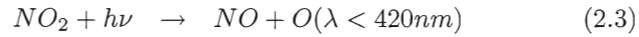
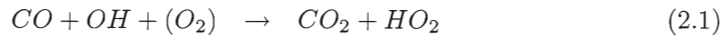
Ozone at the surface comes into direct contact with humans and other living beings and displays its destructive side. Because ozone reacts rapidly with other molecules, high levels of ozone are toxic to living systems. Several studies have documented the harmful effect of ozone on crop production, forest growth and human health. The substantial negative effect of surface-level ozone from this direct toxicity contrasts with the benefits of additional filtering of UV-B radiation that it provides.

## 2.2 Main chemical ozone reaction mechanism

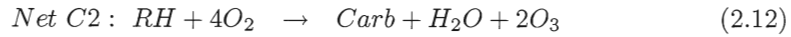
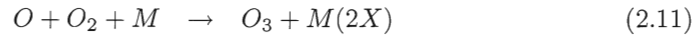
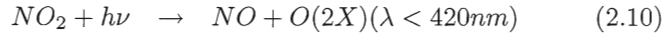
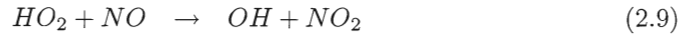
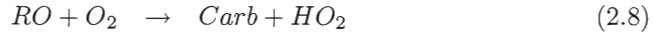
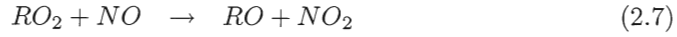
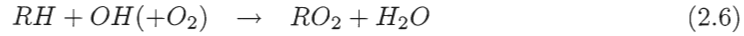
In the atmosphere, ozone is produced and destroyed. The chemical reactions that govern these processes depend on UV light, CO, OH,  $NO_x$  and reactive hydrocarbons. [1]

### 2.2.1 Tropospheric ozone production

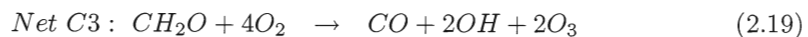
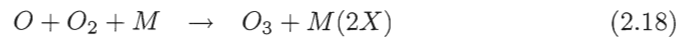
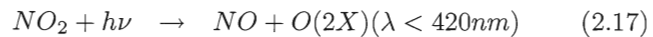
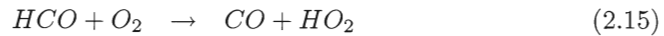
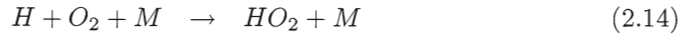
A first photochemical reaction (C1) which produces ozone is the catalytic action of the  $NO_x$  gases in the oxidation chains of CO,  $CH_4$  and other hydrocarbons.



A second photochemical reaction (C2) producing ozone involves the oxidation of hydrocarbons (RH) in the presence of  $NO_x$ , in which NO is oxidized to  $NO_2$  not by  $HO_x$  radicals alone but by reactions with  $HO_2$  and  $RO_2$  radicals, followed by rapid photolysis of  $NO_2$  into NO and O and recombination of O with  $O_2$  to form  $O_3$ . Further degradation of carbonyl compounds (Carb) leads to additional  $RO_2$  and  $HO_2$  formation with ensuing  $O_3$  production.



A third photochemical reaction (C3) responsible for the formation of tropospheric ozone is the oxidation of  $CH_2O$  to CO.  $CH_2O$  is an end product of the total degradation of the carbonyl compounds of reaction C2.



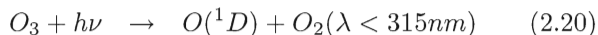


Besides these chemical sources ozone can also be transported from the stratosphere into the troposphere. But this process mainly takes place at extratropical latitudes and near the subtropical jet into the tropics.

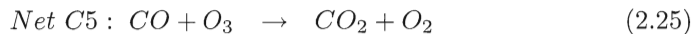
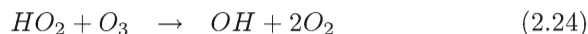
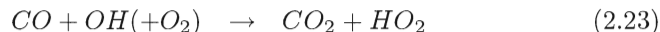
## 2.2.2 Tropospheric ozone destruction

Ozone is destructed in the troposphere, especially near the surface. The main chemical reactions for the destruction process are listed below.

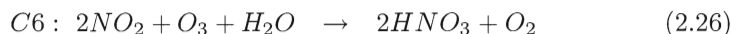
Reaction (C4) is the photo-dissociation of  $O_3$  followed by reaction with water vapour. This reaction not only destroys ozone but is also the main source of the highly reactive hydroxyl (OH) radicals.



Another reaction (C5) responsible for the loss of ozone is the reaction of  $O_3$  with  $HO_2$  radicals. This reaction is part of the the CO oxidation cycle.



In the absence of light photolysis reactions (C1,C2,C3,C4 and C5) do not take place. Reaction (C6) takes place during the night and day and destroys ozone.



## 2.3 Measurement technique

The ozone in the boundary layer near the surface is in situ measured with a photometric ozone analyzer. [12] The UV photometer determines ozone concentration by measuring the attenuation of light due to ozone in the absorption cell, at a wavelength of 254 nm. The concentration is directly related to the magnitude of the attenuation. The reference passes into the absorption cell (A or B figure 2.1) to establish a "zero" light intensity reading ( $I_0$ ). The solenoid then switches, and the sample passes through the absorption cell to establish a "sample" light intensity reading (I). The ratio of these readings ( $I/I_0$ ) is a measure of the light absorbed by ozone in the sample. It is directly related to the concentration of ozone in the sample through the Beer-Lambert law (equation 2.27).

$$\frac{I}{I_0} = e^{-\kappa l C} \quad (2.27)$$

$$K = 308 \text{ cm}^{-1} \text{ at } 0^\circ \text{ C and } 1 \text{ atmosphere}$$

$$l = \text{length of cell, in cm}$$

$$C = \text{mixing ratio}$$

A real time cancellation of potential interferant species occurs via the cyclic process. In the beginning of the cycle, sample enters one cell and reference air (sample with the ozone catalytically removed) enters the second cell. Detectors then measure the light intensity transmitted through each cell. During the second half of the cycle, the roles of the two cells are interchanged by appropriate switching of the solenoid valves. Hence, any absorption of UV energy by chemical species other than ozone are cancelled out. Additionally this balanced optical system serves to correct for fluctuations in lamp intensity and improve response time.

Measurements are taken at 10 seconds intervals and averaged into 10 minutes values. This 10 minutes average is displayed and stored on a computer. The measurement interval of the monitor is set at 0-500 ppbv and the accuracy is 1 ppbv. The inlet of the air sample is situated 3m above the surface and 3m outside the building.

A span-zero check is performed every two days from 9:00 till 10:00 local time. This check serves as calibration of the monitor. During this check a zero gas (ozone free) is supplied at the inlet for 20 minutes, this is for checking the set-off. After this zero-check the span-check is performed. The internal ozonator generates a span gas (high ozone concentration, around 400ppbv), this gas is supplied at the inlet for again 20 minutes. This time the response time and the state of the filter at the inlet are checked.

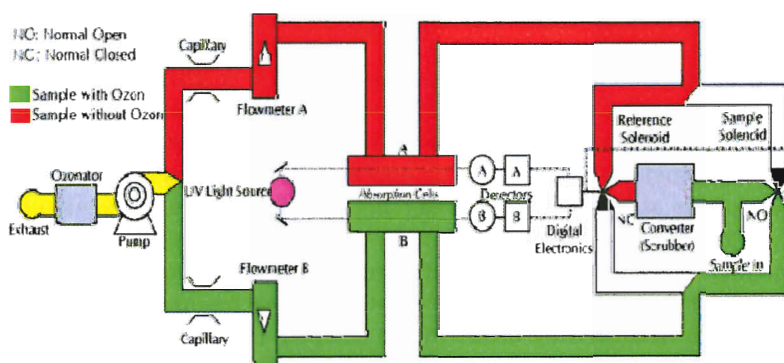


Figure 2.1: Flow diagram of ozonemonitor

## 2.4 Results

Although the data record for the Paramaribo station of surface ozone yet only covers the first 10 months of 2003 (see appendix), a first study of the obtained observational data already shows significant variations on 3 different timescales: diurnal, day-to-day and seasonal.

### 2.4.1 Diurnal variations

The diurnal variation of the surface ozone mixing ratio is helpful in delineating the processes responsible for ozone formation or loss. Figure 2.2 shows the daily dynamics of ozone mixing ratio at the surface.

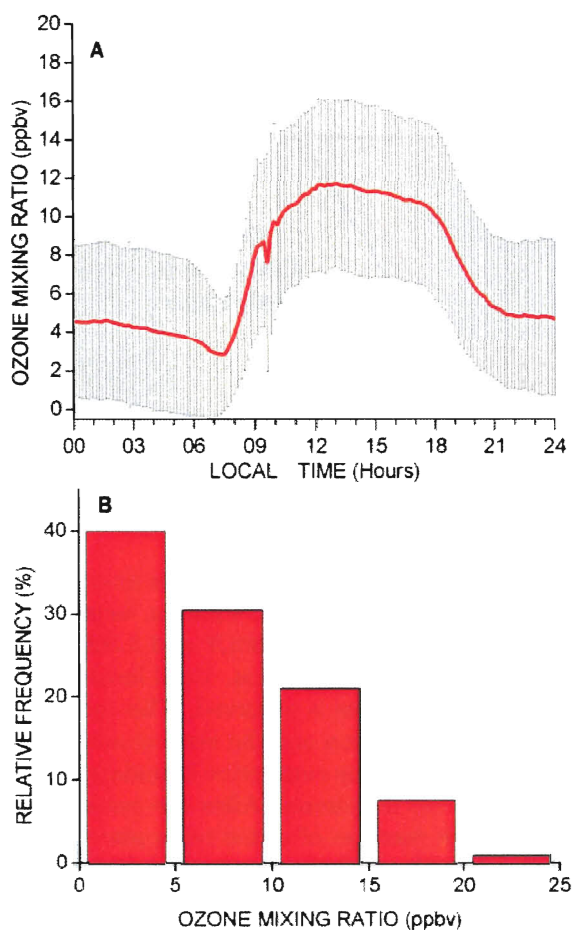


Figure 2.2: Averaged daily surface ozone dynamics Jan-Sep 2003, 10 minute average(A) and relative frequency during measurement period (B).

Ozone mixing ratios exhibit strong diurnal variations. The daily maximum occurs round local noon and the minimum appears in the early morning. Despite the careful filtering of the raw data, there is still an anomaly between 9:00 and 10:00 LT. This is a result of the 2 daily span-zero check. This check is performed to control the accuracy of the ozone monitor.

The diurnal dynamics of the ozone mixing ratios strongly depends on the local dynamic and photochemical effect. During the night the stable nocturnal boundary layer (figure 2.3) uncouples ( typically 300m in depth [13]) from the atmosphere above. After sunset the ozone within this stable nocturnal boundary layer declines as a result of deposition at the surface which depends on the vegetation characteristics [5] and the chemical reaction (C6) of ozone with nitric oxide [3] and [9]. The deposition becomes less effective as the boundary layer becomes more stable in the evening (18:00LT-21:00LT) resulting in a slow decrease of the ozone concentration during the nighttime

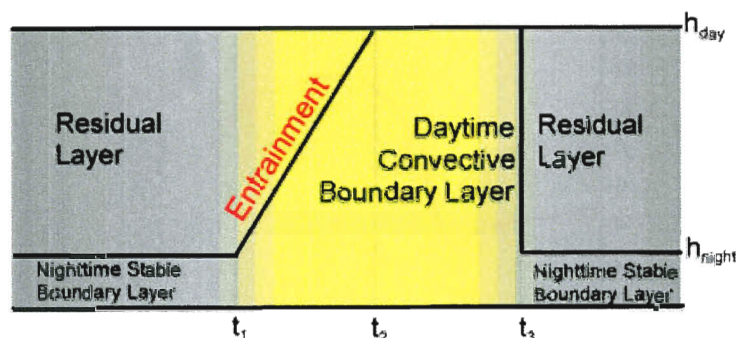


Figure 2.3: Boundary Layer evolution during the day (two-layer model) [13]

From sunrise (6:30LT) till the boundary layer starts growing ( $t_1=7:30\text{LT}$ ), the stable boundary layer breaks up due to solar radiation, causing perhaps the rapid decrease of ozone concentration between 6:30LT and 7:30LT both due to deposition and perhaps photochemical dissociation. Until local noon ( $t_2=13:00\text{LT}$ ) a rapid increase of ozone mixing ratios is observed. This increase may be caused by the local photochemical production and the vertical mixing of ozone from the residual layer aloft when the daytime convective boundary layer starts growing. It is yet unclear which process dominates. After the cessation of the growth of the mixing layer ( $t_2$ ) a slow decrease of ozone takes place. This decrease until the daytime convective boundary layer collapse ( $t_3=18:00\text{LT}$ ) could be caused by a local photochemical reaction (C4), a reaction with isoprene, as well as deposition.

To fully understand the boundary layer budget of ozone more information is required, such as ozone concentration in the free troposphere, isoprene, CO

and  $NO_x$  concentrations in the boundary layer, as well as more information on boundary dynamics throughout the day. This is beyond the scope of this work, but will be the subject of further research.

## 2.4.2 Day-to-day variations

Although the mixing ratio of surface ozone on average is low in the tropics and especially in Surinam, one can distinguish relatively large day-to-day variations. Figure 2.4 shows the day-to-day variation of the daily average ozone mixing ratio at the surface.

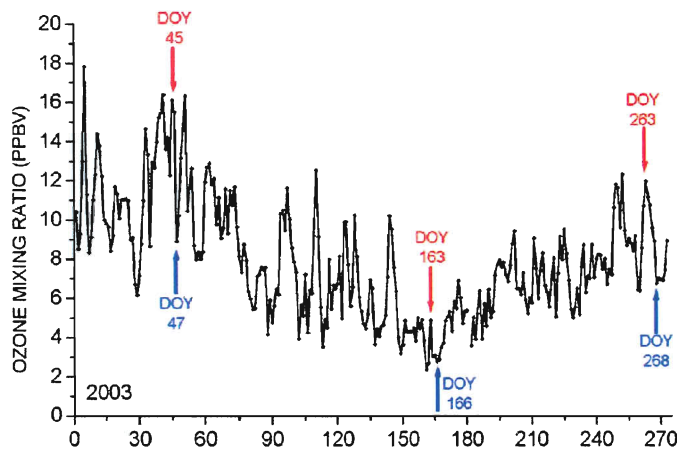


Figure 2.4: Daily average surface ozone concentration. Days indicated are days shown in trajectories (fig 2.5)

A reason for these day-to-day variations could be the origin of the air at the station. As an example the 10 day back 3D trajectories reaching Paramaribo<sup>1</sup> are calculated for 3 cases of significant day-to-day variation. The trajectories prediction of the location of the airmasses 10 days before they cross Paramaribo is more or less the same for the 3 cases. This implies that the relative large variation of the mixing ratio within a couple of days is probably a result of local effects.

Note that the trajectories are consistent with the migration of the ITCZ and the tradewind regimes over Surinam as shown in figure 1.2.

## 2.4.3 Seasonal variations

A full seasonal cycle is not shown in this paper because the data record is not yet complete for the year 2003, as stated before. But one could already distinguish a seasonal variation in the monthly average ozone mixing ratio. Figure

<sup>1</sup>Trajectories based on ECMWF-data and modelled by R. Scheele, KNMI.

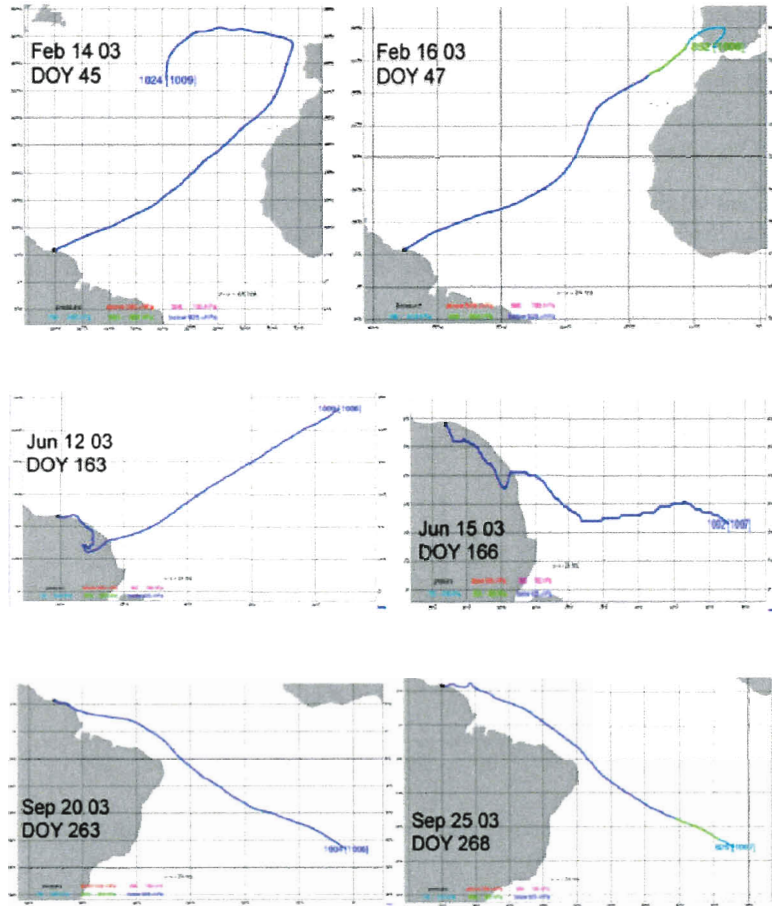


Figure 2.5: 10-day back 3D trajectories reaching Paramaribo at 1010hPa on the dates indicated.

2.6 shows the seasonal variation of the monthly average ozone mixing ratio at the surface in 2003 (first 9 months 2003). The maxima of the mixing ratio occur during the dry seasons. The minima occur during the wet seasons. This can be explained by the fact that during the dry seasons there is more solar insolation than during the wet seasons. And during the long wet season the air is vertically better mixed and pollution is more efficiently removed by wash-out due to the increased precipitation during this period. For instance the airmasses of the June trajectories (figure 2.5) are subject to significant amounts of precipitation and vertical mixing in the 48 hours prior to their arrival over Surinam.

The trajectories of figure 2.5 are related to the seasonal variation in the mixing ratios. In case of the dry seasons, February and September, the air directly

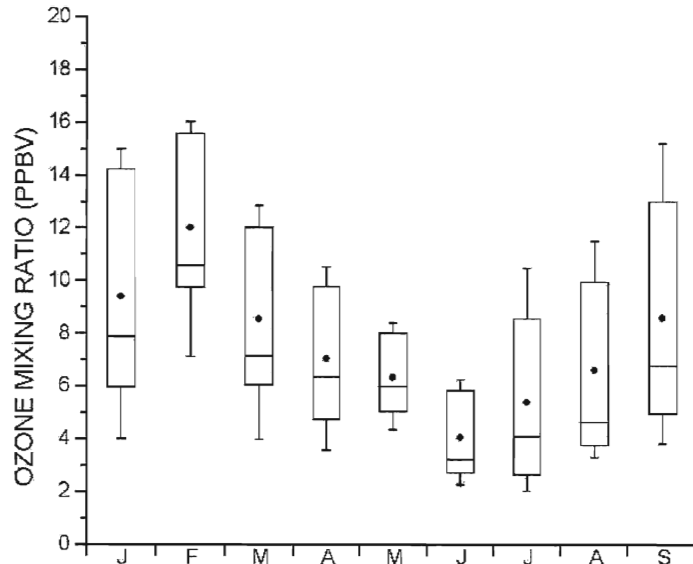


Figure 2.6: The monthly mean (dot), median (bar), inner 50th percentile (box), and inner 90th percentile (whiskers) of the surface ozone mixing ratio from Jan till Sep 2003.

comes from the ocean and is not directly contaminated. During February - March when average mixing ratios are relatively high, it is dry season but also the air comes from the northern hemisphere and could still have increased ozone values and related chemical species, [7], [4] and [2]. In June the airmass is advected over land, but boundary layer concentrations of ozone are extremely low (between 4 and 6 ppbv). It should however be noted that these trajectories are not very accurate since they are passing through regions with to strong convective activity which is only partially taken into account in the calculations.

## 2.5 Discussion and Conclusion

This study of the first observations of ozone surface mixing ratios at Paramaribo station leads to the following conclusions. The measured values of ozone mixing ratios are consistent with other tropical observations. Very low mixing ratios are typical for a tropical site in the nearby of tropical forests. The NE trade winds advect marine air masses over Paramaribo with low ozone concentrations .

The surface ozone mixing ratio exhibits a clear diurnal cycle. This cycle is a result of photochemical reactions and the formation and collapse of the daytime convective boundary layer.

The monthly averaged ozone mixing ratio varies with the seasons. During the wet season a decrease of surface ozone is observed. While during the dry seasons an increase of surface ozone is observed. This could be a result of the more frequently wash-out of ozone and precursors of ozone, a better vertical mixing and less effective photochemical reactions during the wet season.

To have a better understanding of the photochemical processes governing the surface ozone, it is recommended to simultaneously measure CO, isoprene,  $NO_x$  as well as UV measurements. More information on the boundary layer dynamics and the total ozone concentration in the free troposphere is needed to explain the surface ozone variations that are measured.



## Chapter 3

# Cloud Coverage

### 3.1 Introduction

Clouds are involved in chemical processes in the troposphere and play an important part in the global energy budget.

Clouds play a part in atmospheric chemistry. Precipitation is the primary removal mechanism for many atmospheric pollutants. By serving as cloud condensation nuclei (CCN), aerosol particles are incorporated into the cloud droplets and precipitated to the Earth's surface. This process removes most activated condensation nuclei activated and other aerosols that are absorbed through collisions with cloud or rain droplets. The efficiency of washout accounts for the short residence time of tropospheric aerosol. Washout also operates on gaseous pollutants that are water soluble. [10]

Clouds are important for the radiative energy balance of the atmosphere. For LW radiation, the large opacity of clouds increase the optical depth of the atmosphere, which promotes increased surface temperature by enhancing the greenhouse effect. Thus clouds introduce warming in the LW energy budget, and this warming is proportional to the cloud-top temperature. For SW radiation, the high reflectivity of clouds decrease the incoming solar flux, which favors reduced surface temperature. Thus clouds introduce cooling in the SW budget. Unlike the LW effect, cloud albedo is insensitive to cloud height, so low clouds in visible imagery are almost as bright as high clouds. Clouds also introduce heating by absorbing SW radiation.

The overall effect on the surface temperature of clouds is determined by the vertical location of the clouds. High clouds are responsible for surface cooling due to dominance of sunlight reflectance. On the other hand low clouds warm the surface as a result of increased LW downward radiation.

## 3.2 Measurement techniques

### 3.2.1 traditional method

Traditionally, trained human observers have reported cloud overcast conditions. This is done on a scale of 8 (oktas as defined by WMO). Complete cloud cover is reported as 8 oktas, half cover as 4 oktas, and a completely clear sky as zero oktas. If there is low-lying mist or fog, the observer will report sky obscured. The problems with this method are the discrepancies in the data resulting from the subjectivity of the individual observers.

### 3.2.2 Total Sky Imager

The total sky imager (TSI) is a tool for objective observations of the sky. Images from the sky are captured via a solid state CCD imaging camera that looks downward on a heated hemispherical mirror. The mirror images the hemisphere over the system into the lens, and has a solar-ephemeris guided shadowband to block the intense direct-normal radiation from the sun. An imaging processing program samples and saves the captured images to JPEG files for analysis. The same program analyzes the images by first masking out the known obstructions, the camera, its arm, and the sun-blocking shadowband. The raw processed color image is analyzed for fractional cloud cover. The fractional cloud cover is subdivided in opaque and thick. The criteria for the difference between clear, opaque and thick are controlled by two parameters that are set manually.

The values used during the analysis of the first data are set after evaluating several real images and processed images. This is done by comparing processed images with real images for different settings and opting for the settings which generate a processed image most similar to the real image. The entire data set for the results shown are processed with the following parameter settings<sup>1</sup> clear/thin: 75 and thin/opaque: 85.

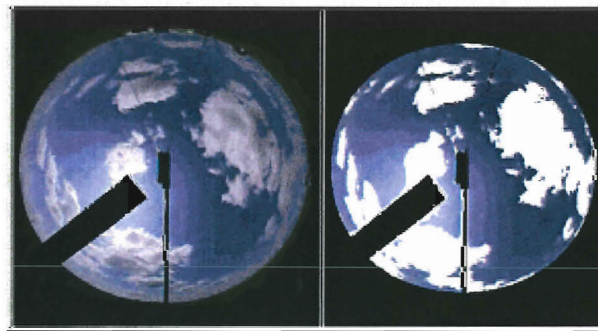


Figure 3.1: left the real image and right the processed image

---

<sup>1</sup>It is unclear what the physical meaning is of these parameters

### 3.2.3 Solar Radiation Station

Another way to determine the cloud coverage is the solar radiation station. At a solar tracker a normal incidence pyrheliometer is attached. This pyrheliometer measures the normal incidence direct solar radiance from 200nm till 4000nm. The processed data of the station gives an indication of the sun duration. The sun duration is defined as the fraction of time when the normal incidence radiation is higher than  $150 \text{ W/m}^2$ . The method therefore only works when the clear sky radiation is significantly higher than  $150 \text{ W/m}^2$ , which is roughly between 9:00 and 17:00 LT (12:00 and 20:00 GMT). The data processing software defines sun duration zero when the irradiance is lower than  $150 \text{ W/m}^2$  (corrected for the angle of incidence) gradually, with steps of 0.1, it goes to a value of one for a clear sky. Thus the sun duration is an indicator of the cloud coverage. The relation between the sun duration and cloud coverage is  $100 - \% \text{ sunduration} * 100 = \% \text{ cloud coverage}$ .

## 3.3 Results

### 3.3.1 Comparison TSI-RS

The results for the daily average cloud coverage of the first 2 months of 2003 is shown in figure 3.2 for both measurement techniques and the absolute value of the difference between TSI-data and RS-data.

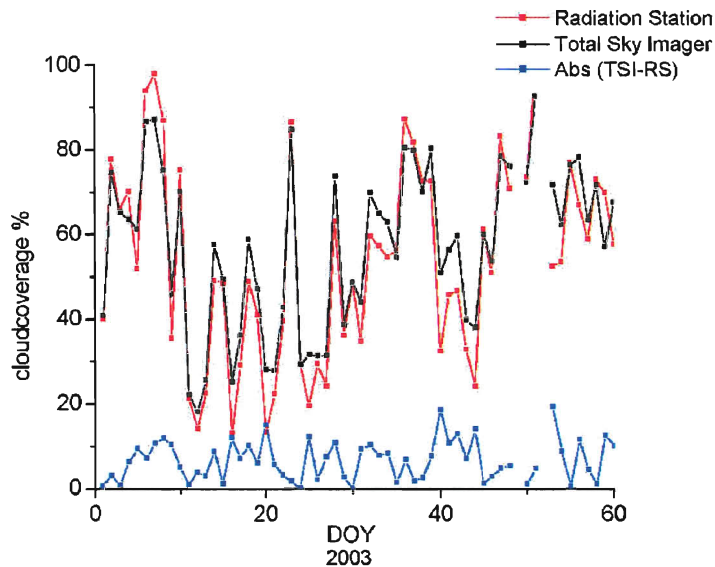


Figure 3.2: daily average cloud coverage at Paramaribo Station Jan-Feb 2003

The two measurement techniques show the same day-to-day variations. The difference between the daily averaged cloud coverage obtained with the TSI and RS is less than 20% for all days and less than 10% for more than 75% of the days. For values greater than 70 % the RS-values are always larger than the TSI values. The RS data smaller than 30% are likewise always smaller than the TSI data. For values between 30% and 70% the TSI values are larger than the RS values. The reason for these differences can be found in the fact that the RS covers one spot in the sky while the TSI covers the whole sky and therefore the latter shows a more averaged signal. On days with a half covered sky (a cloud coverage around 50 %), the TSI detects more clouds than the RS. This could be a result of the anomaly resulting from the 2D projection of the 3D clouds. A slant view of the sky will produce an error (to high cloud covers), when the sky is covered with scattered cumulus towers. Therefore the RS which primarily focuses on the sun detects less clouds than the TSI.

### 3.3.2 Diurnal variation

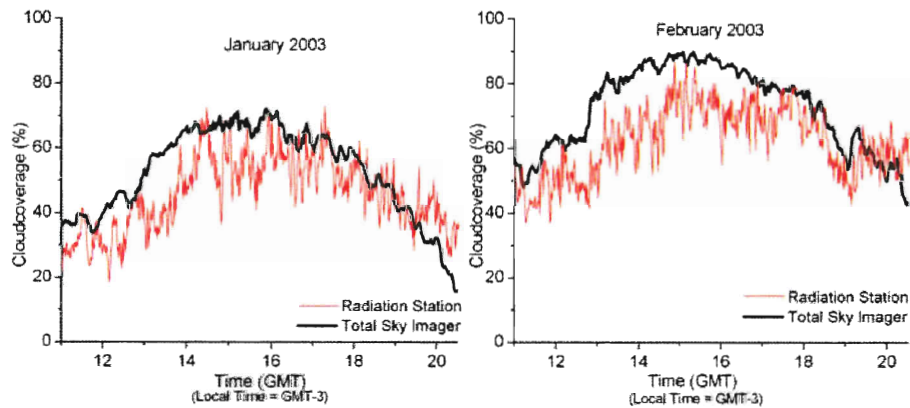


Figure 3.3: averaged diurnal variation of cloud cover over Paramaribo during January and February 2003

The diurnal variations of the two measurement techniques show the same pattern. The RS-data has more variation than the TSI-data, for reasons given above.

The diurnal variations of the cloud cover over Paramaribo station shows the same diurnal pattern as derived from satellite data observed above tropical area. The maximum of the cloud coverage occurs at 15:00 GMT which is also described by [11].

The accuracy of the two methods differ 9%. The TSI data has an accuracy of 1% and the RS of 10%. This explains the bigger variations on the averaged diurnal cloud coverage of the RS data compared to the TSI values.

### 3.4 Discussion and Conclusion

The cloud coverage measurements made with the Total Sky Imager and the derived cloud coverage of the solar radiation station are in good agreement. The TSI results are more spatially averaged than the RS measurements. Therefore the TSI is the correct method for the cloud coverage measurements. It is recommended to obtain better understanding of the physical meaning of the parameter settings in the TSI data analysis software.

The measured diurnal dynamics of the cloud coverage are typical for tropical areas. [11] To get a better picture of the variations of the cloud coverage on different timescales extensive data analysis is recommended.

The new objective measuring methods for cloud coverage are an asset for the Paramaribo station. These new data sets will be valuable for model validation and a better understanding of the tropical atmosphere.



# Bibliography

- [1] J.P. Crutzen. *Composition, Chemistry and Climate of the Atmosphere*, chapter Ozone in the Troposphere. von Nostrand Reinhold, 1995.
- [2] J. de la Cruz, J.M. Martin-Gonzalez, and P. Sancho. Surface ozone measurements at tairte, gran canaria (canary islands, spain). *IL NUOVO CIMENTO*, 20(2):181–194, March-April 1997.
- [3] M.A.F. Silva Dias, S. Rutledge, P. Kabat, P.L. Silva Dias, C.Nobre, G. Fisch, A.J. Dolman, E. Zipser, M. Garstang, A. Manzi, J.D. Fuentes, H. Rocha, J. Marengo, A. Plana-Fattori, L. Sa, R. Alvala, M.O. Andreae, P. Artaxo, R. Gielow, and L. Gatti. Cloud and rain processes in a biosphere interaction context in the amazon region. *Journal of Geophysical Research - Atmosphere*, LBA special issue, June 2001.
- [4] G.L. Gregory, E.V. Browell, and L.S. Warren. Boundary layer ozone: An airborne survey above the amazon basin. *Journal of Geophysical Research*, 93(D2):1452–1468, February 1988.
- [5] V.W.J.H. Kirchhoff. Surface ozone measurements in amazonia. *Journal of Geophysical Research*, 93(D2):1469–1476, February 1988.
- [6] J. Lelieveld and A.M. Thompson. *Scientific Assessment of Ozone Depletion: 1998*, chapter FAQ about Ozone. Number 44. World Meteorological Organization, 1998.
- [7] S.J. Oltmans and H. Levy II. Surface ozone measurements from a global network. *Atmospheric environment*, 28(1):9–24, January 1994.
- [8] W. Peters. *Ozone in the Tropical Troposphere*. PhD thesis, Universiteit Utrecht, December 2002.
- [9] P. Pochanart, H. Akimoto, P. Sukasem, Y. Kajii, and S. Kato. Regional ozone and carbon monoxide in southeast asia from observation in thailand. <http://ies.jrc.cec.eu.int/Units/cc/events/torino2001/torinocd/Documents/Urban/UO3.htm>, 2001.
- [10] M.L. Salby. *Fundamentals of Atmospheric Physics*, volume 61 of *International Geophysics Series*. Academic Press, 1996.

- [11] J. Schmetz, K. Holmlund, M. Konig, and H.-J. Lutz. Observation of the diurnal variation of upper tropospheric divergence in a tropical convective system. website: [http://www.eumetstat.de/eu/areaz/proceedings/eum35/sessionz/Schemtz\\_final.pdf](http://www.eumetstat.de/eu/areaz/proceedings/eum35/sessionz/Schemtz_final.pdf), 2001.
- [12] Thermo Electron Corporation, Environmental Instruments Division, Massachusetts, USA. *MODEL 49/49PS, U.V. Photometric Ambient Ozone Analyzer/Calibrator, INSTRUCTION MANUAL*, April 1991.
- [13] G. Verver. *Interactions of Mixing and Chemistry in the Atmospheric Boundary Layer*. PhD thesis, Universiteit Utrecht, November 1999.



# Appendix

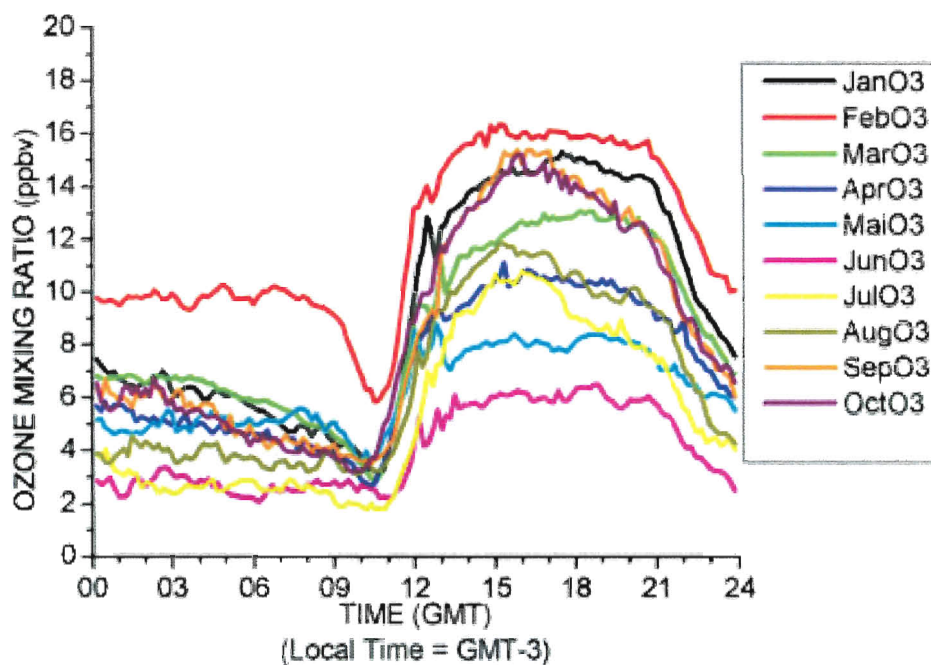


Figure 3.1: Averaged daily surface ozone dynamics for first 10 months of 2003

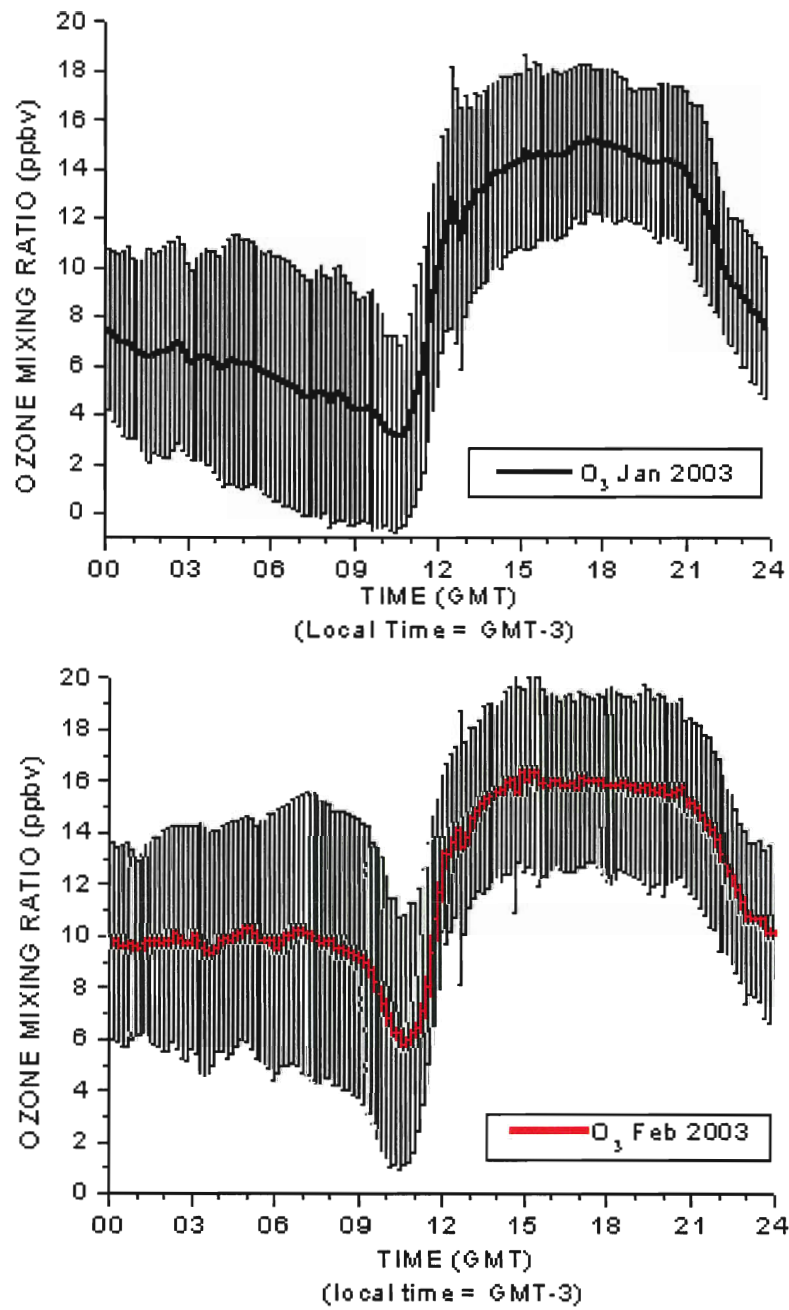


Figure 3.2: Averaged daily surface ozone dynamics for January and February 2003

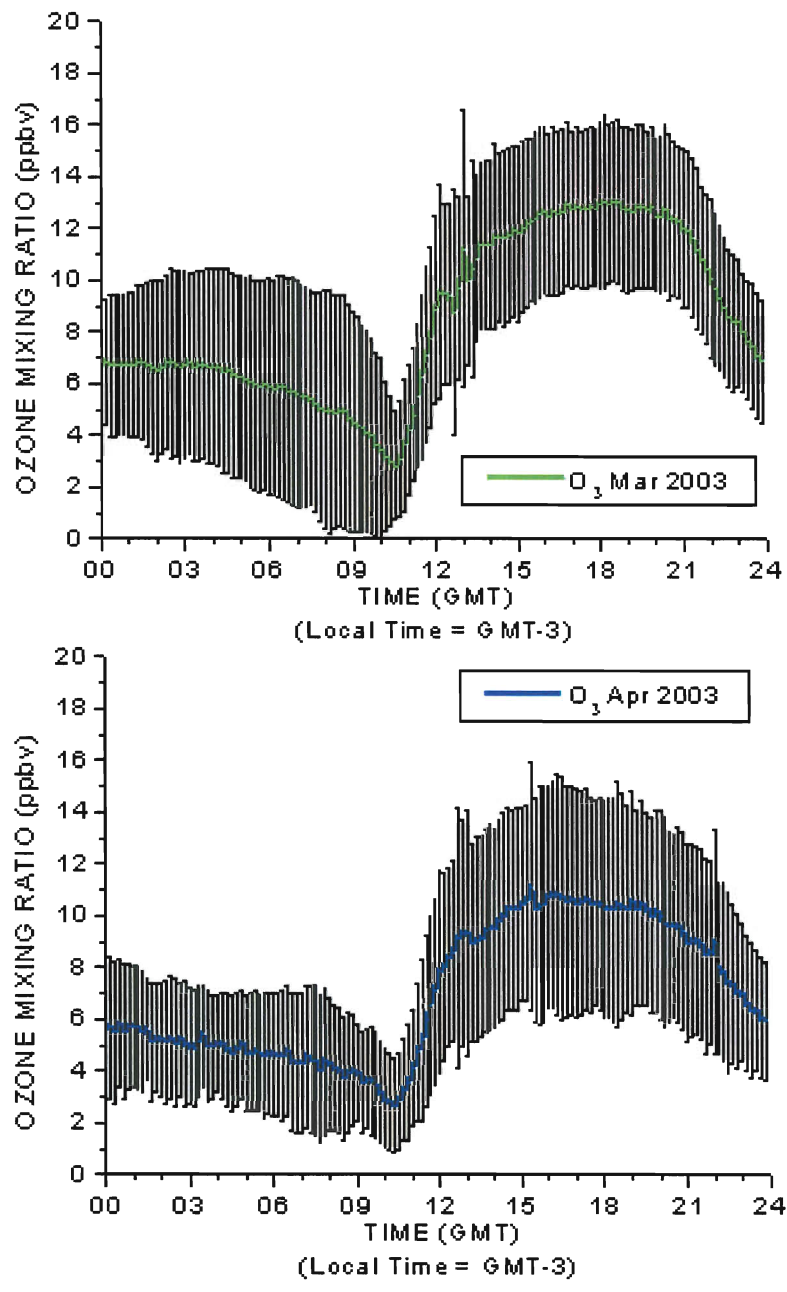


Figure 3.3: Averaged daily surface ozone dynamics for March and April 2003

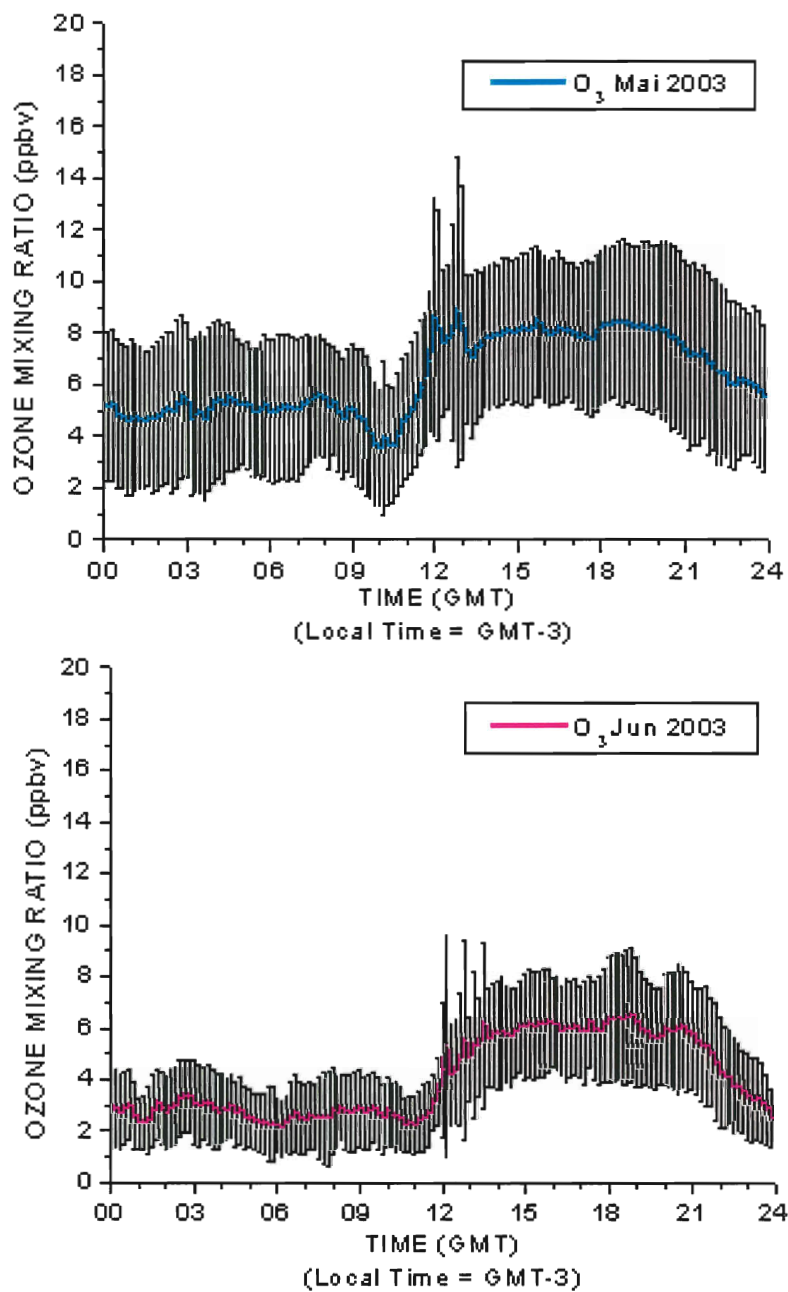


Figure 3.4: Averaged daily surface ozone dynamics for May and June 2003

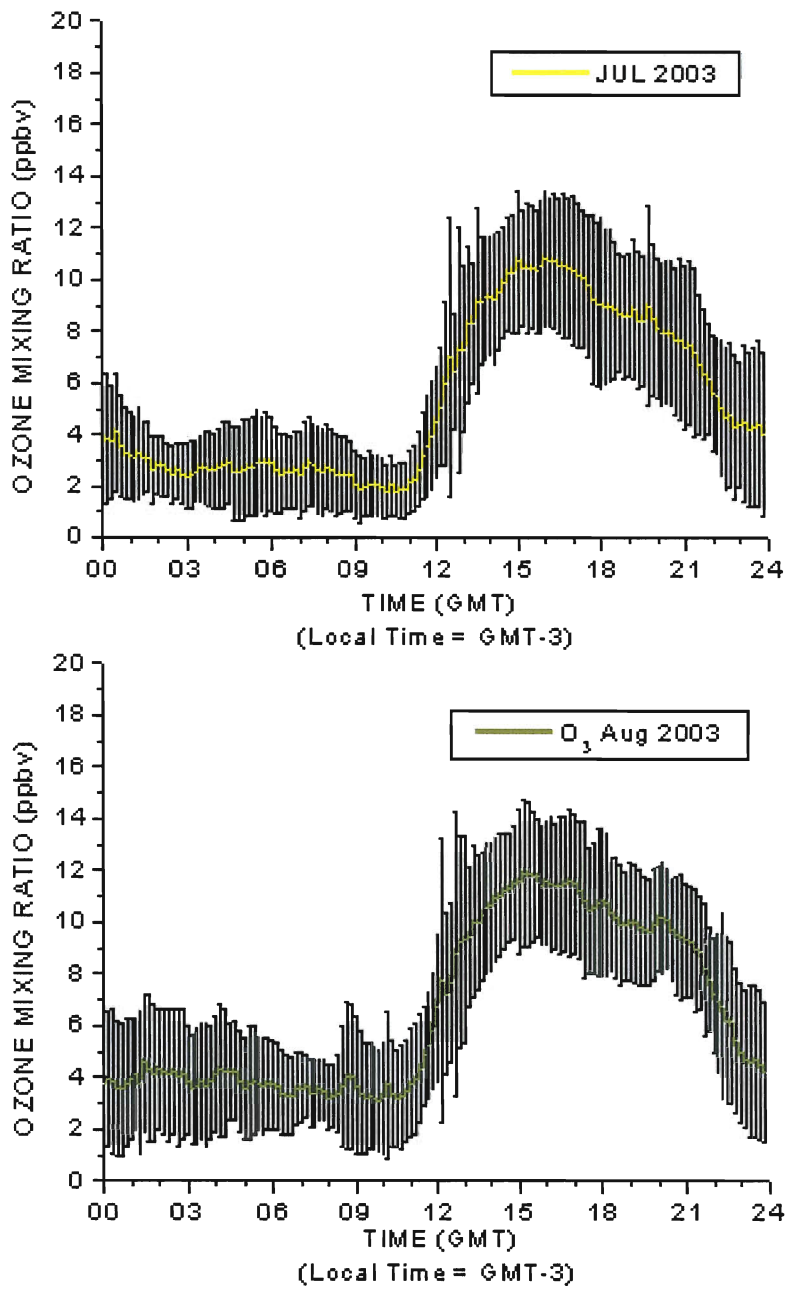


Figure 3.5: Averaged daily surface ozone dynamics for July and August 2003

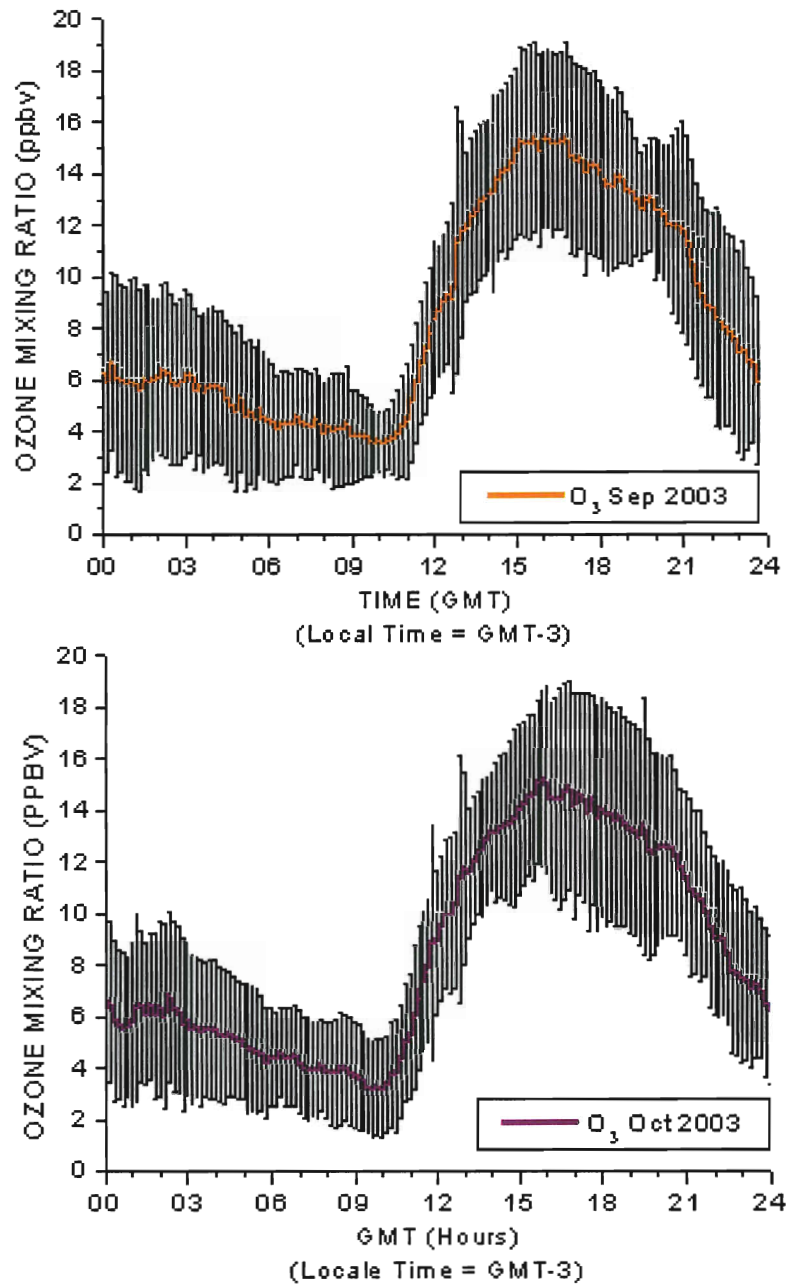


Figure 3.6: Averaged daily surface ozone dynamics for September and October 2003



